

Comparison of predicted ferromagnetic tendencies of Mn substituting the Ga site in III-V's and in I-III-VI 2 chalcopyrite semiconductors

Yu-Jun Zhao, Priya Mahadevan, and Alex Zunger

Citation: [Applied Physics Letters](#) **84**, 3753 (2004); doi: 10.1063/1.1737466

View online: <http://dx.doi.org/10.1063/1.1737466>

View Table of Contents: <http://scitation.aip.org/content/aip/journal/apl/84/19?ver=pdfcov>

Published by the [AIP Publishing](#)

Articles you may be interested in

[Ferromagnetism of low-dimensional Mn-doped III-V semiconductor structures in the vicinity of the insulator-metal transition](#)

[J. Appl. Phys.](#) **107**, 023905 (2010); 10.1063/1.3267314

[Transition from ferromagnetism to antiferromagnetism in Ga \$1-x\$ Mn \$x\$ N](#)

[J. Appl. Phys.](#) **98**, 083905 (2005); 10.1063/1.2115091

[Local structure and chemical valency of Mn impurities in wide-band-gap III-V magnetic alloy semiconductors Ga \$1-x\$ Mn \$x\$ N](#)

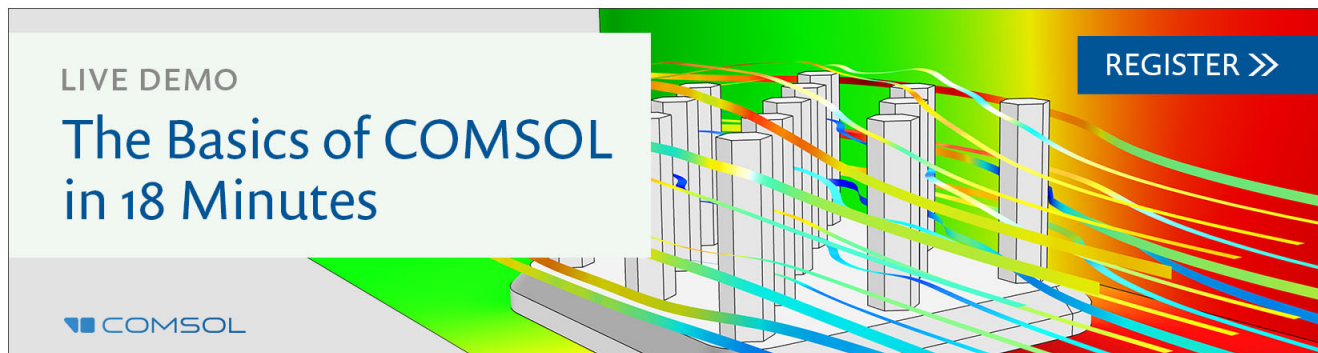
[Appl. Phys. Lett.](#) **79**, 3926 (2001); 10.1063/1.1423406

[Ferromagnetic phenomenon revealed in the chalcopyrite semiconductor CdGeP₂: Mn](#)

[J. Appl. Phys.](#) **89**, 7027 (2001); 10.1063/1.1357842

[Limits on the Curie temperature of \(III,Mn\)V ferromagnetic semiconductors](#)

[Appl. Phys. Lett.](#) **78**, 1550 (2001); 10.1063/1.1355300

A promotional banner for COMSOL software. On the left, a white box contains the text 'LIVE DEMO' and 'The Basics of COMSOL in 18 Minutes'. The COMSOL logo is at the bottom left. The background features a 3D bar chart with colorful, flowing lines representing data or simulation results. A blue button with the text 'REGISTER >>' is located in the top right corner.

LIVE DEMO

The Basics of COMSOL in 18 Minutes

COMSOL

REGISTER >>

Comparison of predicted ferromagnetic tendencies of Mn substituting the Ga site in III–V's and in I–III–VI₂ chalcopyrite semiconductors

Yu-Jun Zhao, Priya Mahadevan, and Alex Zunger^{a)}

National Renewable Energy Laboratory, Golden, Colorado 80401

(Received 5 December 2003; accepted 9 March 2004; published online 29 April 2004)

We report density-functional calculations of the ferromagnetic (FM) stabilization energy $\delta = E_{\text{FM}} - E_{\text{AFM}}$ for differently oriented Mn pairs in III–V's (GaN, GaP, GaAs) and chalcopyrite (CuGaS₂, CuGaSe₂, CuGaTe₂) semiconductors. Ferromagnetism is found to be the universal ground state ($\delta < 0$) in all cases. The order of FM stability in III–V's is GaN > GaP > GaAs, whereas in chalcopyrites it is CuGaS₂ > CuGaSe₂ > CuGaTe₂. Considering both groups, the order is GaN → GaP → GaAs → CuGaS₂ → CuGaSe₂ → GaSb ≈ CuGaTe₂. The stronger FM stabilization in III–V's is attributed to the stronger covalent coupling between the Mn 3*d* and the anion *p* orbitals. In contrast to expectations based on Ruderman–Kittel–(Kasuya)–Yosida, (i) all Mn–Mn pair separations show FM, with no FM to antiferromagnetic oscillations and, (ii) FM is orientationally dependent, with $\langle 110 \rangle$ Mn–Mn pairs being the most FM. © 2004 American Institute of Physics. [DOI: 10.1063/1.1737466]

Substitution of the trivalent Ga site in III–V semiconductors by divalent Mn creates a hole which mediates ferromagnetic interactions between the *d*⁵ spins of the Mn ions.^{1,2} The *n*-type doping (e.g., via Mn interstitials^{3–5} or As antisites^{5–7}) compensates the holes, thereby weakening or even removing the ferromagnetism. The search for Ga-containing host semiconductors which are not *n* type has largely focused so far on GaN,⁸ GaP,⁹ and GaAs,¹⁰ leading, however, to rather low ferromagnetic transition temperatures (in GaAs),¹⁰ or to the unwanted precipitation of competing phase (in GaN).^{11,12} Here we inquire whether another class of Ga-containing semiconductors could be interesting for Mn-induced ferromagnetism, namely I–III–VI₂ chalcopyrite. Previous calculations^{13–15} have shown promise. Here we will contrast the calculated ferromagnetic stabilization energy $\delta = E_{\text{FM}} - E_{\text{AFM}}$ for Mn ions in chalcopyrite and in III–V's by comparing, via density functional theory, the total energies *E* of supercells in ferromagnetic (FM) and antiferromagnetic (AFM) spin arrangements. We find that for low concentration of Mn (i) both classes of materials show $\delta < 0$, i.e., FM is the ground state. (ii) The most negative stabilization energy occurs when the Mn ions are located along the $\langle 110 \rangle$ chain connecting in III–V's the atoms Ga–As–Ga–As–⋯, and in I–III–VI₂ the atoms Cu–Se–Ga–Se–⋯. (iii) In III–V's, the strength of ferromagnetism (e.g., for the first-neighbor Mn atoms) decreases along the series GaN → GaP → GaAs → GaSb, whereas in chalcopyrite it decreases along the series CuGaS₂ → CuGaSe₂ → CuGaTe₂. Finally, (iv) comparing all compounds, the FM stability decreases along GaN → GaP → GaAs → CuGaS₂ → CuGaSe₂ → GaSb ≈ CuGaTe₂. We have previously shown^{4,16} that ferromagnetism in this compounds results from direct Mn 3*d* coupling with the anion *p* orbital, not from the Ruderman–Kittel–(Kasuya)–Yosida (RK(K)Y) coupling. The sequence of FM stability above reflects the magnitude of this coupling.

We use 64-atom supercells, placing one Mn at (0,0,0)*a* and the second in various lattice positions, such as $(\frac{1}{2}, 0, \eta/2)a$, (1,0,0)*a*, $(\frac{1}{2}, \frac{1}{2}, \eta)a$, and (1,1,0)*a*, in III–V's and chalcopyrites, corresponding to first, second, third, and fourth neighbors, respectively. Here the tetragonal ratio η is *c*/2*a*, and equals 1 in the cubic III–V's. All atomic positions and lattice constants are relaxed by minimizing the energy as calculated by plane-wave pseudopotential total-energy momentum space method,¹⁷ using the ultrasoft pseudopotentials of Vanderbilt,¹⁸ and the generalized gradient approximation (GGA) to the exchange correlation¹⁹ as implemented in the VASP code.²⁰ The plane-wave basis set had a cutoff energy of 13.3 Ry for GaSb, GaAs, and GaP, 29.4 Ry for GaN, and 21.5 Ry for the chalcopyrites, and a shifted Monkhorst–Pack grid²¹ of 4 × 4 × 4 *k* points including Γ was employed. The magnetic stabilization energy δ is converged to within 4 meV when the sampling *k* mesh is increased to 6 × 6 × 6 or the energy cutoff is increased by 30%.

Figure 1 compares the Mn 3*d* density of states (DOS) of GaAs:Mn with CuGaSe₂:Mn. Going from low energy to high energy, and labeling states according to tetrahedral representations (*t*₂ or *e*), spin (up or down; + and –, respectively), and type of states [“dangling bond hybrid” (DBH), or “crystal field resonance” (CFR) as a result of bonding and antibonding interaction between Mn *d* states and the anion dangling bond states], we find the same order for GaAs:Mn and CuGaSe₂:Mn²²

$$t_{+}^{\text{CFR}} < e_{+}^{\text{CFR}} < t_{-}^{\text{DBH}} < t_{+}^{\text{DBH}} < e_{-}^{\text{CFR}} < t_{-}^{\text{CFR}}. \quad (1)$$

The *t*^{DBH} states represent the states mostly localized at anion sites. On the other hand, the *e*^{CFR} and *t*^{CFR} states are mostly Mn-localized states. (The level ordering may be different for other III–V's and I–III–V₂'s. For example, the DBH levels are lower than all the CFR levels in GaN:Mn,^{23,24} and *e*₊^{CFR} < *t*₊^{CFR} in CuAlS₂:Mn.¹⁵) The order of states in Eq. (1) can

^{a)}Author to whom correspondence should be addressed; electronic mail: azunger@nrel.gov

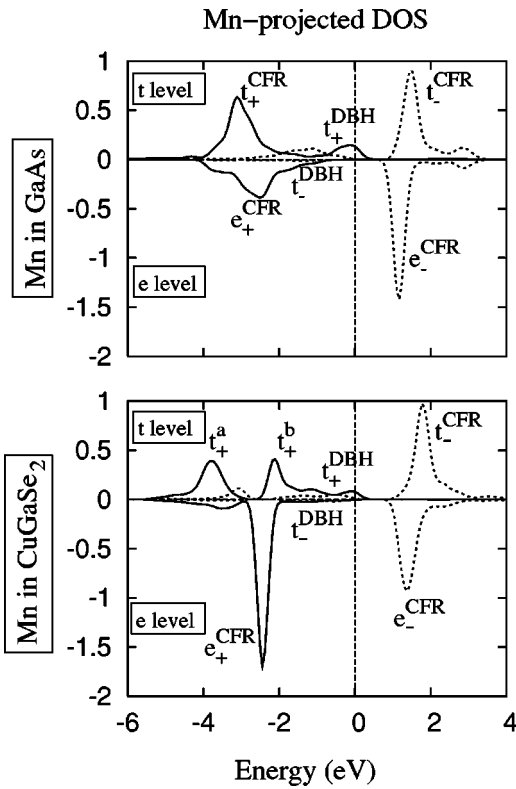


FIG. 1. Projected e and t DOS levels for Mn_{Ga} in GaAs and CuGaSe₂ in a sphere radius of 1.20 Å. Spin up DOS is shown in solid lines, whereas spin-down in dashed line. The Fermi level is set to zero.

be explained by a simple model,^{4,16,25} depicted in Fig. 2. We describe the electronic structure of Mn_{Ga} as a result of coupling between the d orbitals of the Mn ion with the orbitals formed by a Ga vacancy in CuGaSe₂ or GaAs. The d orbitals of a Mn^{2+} ion, are split into $e(d) + t_2(d)$ by the point-ion crystal field and into up spin (e_+, t_+) and down spin (e_-, t_-) via the exchange interaction. The vacancy orbitals $t_2(p)$ are actually dangling bonds of the anions surrounding the vacant Ga site. Calculation of V_{Ga} in CuGaSe₂ show that at Γ , the $t_2(p)$ vacancy level is at $E_{\text{VBM}} + 40$ meV, i.e.,

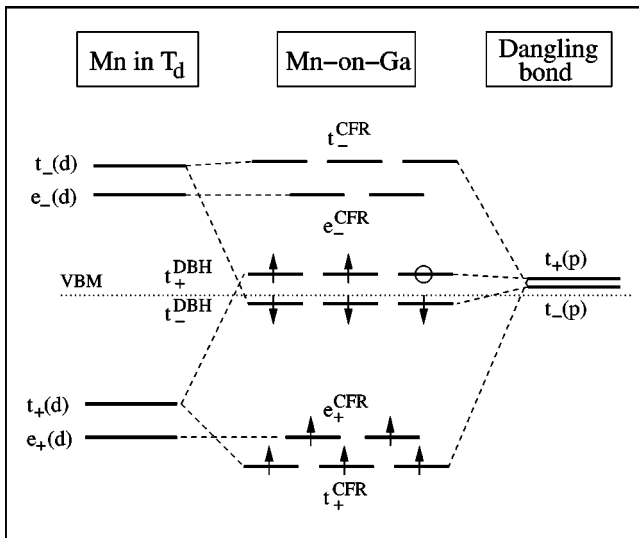


FIG. 2. The energy level diagram of Mn in GaAs and CuGaSe₂. The level splitting due to the tetragonal structure in CuGaSe₂ is not shown in this figure.

TABLE I. Comparison of ferromagnetic stability energy $\delta = E_{\text{FM}} - E_{\text{AFM}}$ (meV/Mn) for two Mn_{Ga} pairs in a 64-atom supercell in III-V and I-III-VI₂ semiconductors. One Mn is located at $(0,0,0)a$, while the other is located as listed in the table ($\eta = c/2a$).

System	δ for different Mn-Mn pairs			
	$(\frac{1}{2}, 0, \frac{\eta}{2})a$	$(1,0,0)a$	$(\frac{1}{2}, \frac{1}{2}, \eta)a$	$(1,1,0)a$
GaN (ZB)	-188	-11	-63	-161
GaP	-139	-31	-89	-132
GaAs	-124	-30	-76	-114
GaSb	-56	-7	-28	-54
CuGaS ₂	-81			-83
CuGaSe ₂	-71			-61
CuGaTe ₂	-52			-59

slightly above the valence band minimum (VBM). If this energy of the cation vacancy lies between the energies of up-spin and the down-spin Mn 3d orbitals (Fig. 2), one obtains a level scheme as shown at the center panel of Fig. 2. The spin-up Mn orbital $t_+(d)$ hybridizes with the spin-up dangling bond $t_+(p)$, to form the bonding $t_+^{\text{CFR}}(dp)$ and the anti-bonding $t_+^{\text{DBH}}(dp)$ levels. The bonding orbital contains mostly $t_+(d)$ character, whereas the anti-bonding orbital contains more $t_+(p)$ character. Analogously, the spin-down Mn orbital $t_-(d)$ hybridizes with the spin-down host dangling bond $t_-(p)$ to form the bonding $t_-^{\text{CFR}}(dp)$ and the anti-bonding $t_-^{\text{DBH}}(dp)$. The coupling matrix element $|V_{pd}|$ increases with covalency and with the reduction in bond length. Note that t_-^{DBH} is below t_+^{DBH} (“negative DBH exchange splitting”) since t_-^{DBH} is repelled downward [by $t_-(d)$] more than t_+^{DBH} is repelled upward [by $t_+(d)$]. In contrast, t_+^{CFR} is below t_-^{CFR} (“positive CFR exchange splitting”). Thus, the direction of spin polarization on the Mn site (decided by CFR) is opposite to the direction of spin polarization on the nearest anion sites (decided by DBH). This is the fingerprint of antiferromagnetic coupling between Mn 3d and the anion p orbitals. Since the host dangling bonds do not have an e -like representation in the relevant energy range, the Mn $e_-(d)$ and $e_+(d)$ levels are mostly unperturbed, and appear as e_-^{CFR} and e_+^{CFR} . Note that the t_+^{CFR} level is now lower than the e_+^{CFR} level (opposite to what a point-ion crystal-field theory would suggest) due to bonding with the DBH. Thus, the simple model of Fig. 2 reproduces the essential feature (e.g., level ordering) of the full first-principles calculations, and shows that the hole at the Fermi level resides in a spin-up dangling bond hybrid, t_+^{DBH} .

Table I shows the ferromagnetic stabilization energy δ for pairs of Mn ions in III-V’s and in I-III-VI₂ chalcopyrites. We see that in all cases, substitution of the column III site leads to ferromagnetism ($\delta < 0$). This is because of the occurrence of a t_-^{DBH} hole in both systems. The strength of the stabilization energy depends on the crystallographic orientation and interatomic separation of the two Mn atoms. In sharp contrast with the expectation from the RK(K)Y model,²⁶ all Mn-Mn separations up to fourth nearest neighbor show only ferromagnetic behavior with no FM/AFM oscillations. The orientation dependence [not expected by RK(K)Y] is such that $\langle 110 \rangle$ -oriented Mn-Mn pairs, [e.g., the first neighbor being $(\frac{1}{2}, \frac{1}{2}, 0)a - (0,0,0)a$ pair and the fourth

neighbor being $(1,1,0)a-(0,0,0)a$ pair] have the highest FM stability. This crystallographic orientation has the strongest coupling between t^{DBH} on adjacent Mn–As bonds since it is the only direction where *bond chains* occur, i.e., like Ga–As–Ga–As– \cdots in III–V's, or Cu–Se–Ga–Se– \cdots in chalcopyrites.

We next compare our calculated stability energies δ with results in literature. For example, using GGA exchange correlation and relaxed lattice constant we obtained -188 and -63 meV/Mn for Mn pairs of first neighbors and third neighbors in GaN:Mn, respectively, while Sanyal, Bengone, and Mirbt give -156 and -58 meV/Mn, respectively, employing local density approximation (LDA) and experimental lattice constant.²⁴ As for the GaAs:Mn, Ref. 24 presented $\delta = -130$ meV/Mn for nearest neighbor pair of Mn, which is in good agreement with ours (-124 meV/Mn). However, for the second nearest neighbor Mn pair, our δ value (-30 meV/Mn) is much smaller than that in Ref. 24 (-70 meV/Mn), while Ref. 27 also gives -30 meV/Mn using LDA. In addition, Sanyal and co-workers, concluded that the ferromagnetic interaction in GaN:Mn is short ranged²⁴ without considering the Mn pair separated by $(1,1,0)a$. In fact, the interaction for Mn pair of fourth neighbor is very strong (c.f. Table I).

The order of FM stability (absolute value of δ), e.g., for the first nearest neighbor and fourth nearest neighbor among III–V's is GaN>GaP>GaAs>GaSb, whereas in the chalcopyrites it is CuGaS₂>CuGaSe₂>CuGaTe₂. Comparing all compounds, we find that GaN:Mn, GaP:Mn, and GaAs:Mn have stronger FM stability than all the studied chalcopyrites. Ferromagnetism in GaSb:Mn is comparable to that in CuGaTe₂:Mn, but weaker than CuGaS₂:Mn and CuGaSe₂:Mn. Since the anion (column VI) in chalcopyrites is more ionic than the anion (column V) in III–V's, the covalent bonding V_{pd} between Mn $3d$ and anion p , and thus the AFM coupling, is weaker in chalcopyrites, resulting in a weaker FM stabilization. This is evidenced by the fact that the magnetic moments in the As sphere in GaAs:Mn ($0.035 \mu_B$ within $R=1.2 \text{ \AA}$), are much higher than that in the Se sphere ($0.003 \mu_B$ within $R=1.2 \text{ \AA}$) of CuGaSe₂:Mn, which indicates the stronger AFM coupling in III–V's. The strength of covalent coupling V_{pd} is partially reflected in the band gaps. Individually, within the III–V or the chalcopyrite series, the FM stability scales consistently with the energy gap. However, this is no longer the case considering both III–V's and chalcopyrites. For example, CuGaS₂ has an energy gap

of 2.43 eV, being larger than that of GaP (2.26 eV) or GaAs (1.43 eV), yet the FM stability of CuGaS₂:Mn is weaker than in GaP:Mn or GaAs:Mn. Indeed, III–V's have stabler ferromagnetism than chalcopyrites for comparable energy gaps.

The authors acknowledge support of this work by the Office of Naval Research (ONR).

- ¹H. Ohno, *Science* **281**, 951 (1998).
- ²S. A. Wolf, D. D. Awschalom, R. A. Buhrman, J. M. Daughton, S. von Molnr, M. L. Roukes, A. Y. Chtchelkanova, and D. M. Treger, *Science* **294**, 1488 (2001).
- ³S. C. Erwin and A. G. Petukhov, *Phys. Rev. Lett.* **89**, 227201 (2002).
- ⁴P. Mahadevan and A. Zunger, *Phys. Rev. B* **68**, 075202 (2003).
- ⁵L. Bergqvist, P. A. Korzhavyi, B. Sanyal, S. Mirbt, I. A. Abrikosov, L. Nordström, E. A. Smirnova, P. Mohn, P. Svedlindh, and O. Eriksson, *Phys. Rev. B* **67**, 205201 (2003).
- ⁶S. Sanvito and N. A. Hill, *Appl. Phys. Lett.* **78**, 3493 (2001).
- ⁷T. E. M. Staab, R. M. Nieminen, J. Gebauer, R. Krause-Rehberg, M. Luysberg, M. Haugk, and T. Frauenheim, *Phys. Rev. Lett.* **87**, 045504 (2002).
- ⁸T. Sasaki, S. Sonoda, Y. Yamamoto, K. Suga, S. Shimizu, K. Kindo, and H. Hori, *J. Appl. Phys.* **91**, 7911 (2002).
- ⁹E. Tarhan, I. Miotkowski, S. Rodriguez, and A. K. Ramdas, *Phys. Rev. B* **67**, 195202 (2003).
- ¹⁰H. Ohno, A. Shen, F. Matsukura, A. Oiwa, A. Endo, S. Katsumoto, and Y. Iye, *Appl. Phys. Lett.* **69**, 363 (1996).
- ¹¹B. K. Rao and P. Jena, *Phys. Rev. Lett.* **89**, 185504 (2002).
- ¹²S. S. A. Seo, M. W. Kim, Y. S. Lee, T. W. Noh, Y. D. Park, G. T. Thaler, M. E. Overberg, C. R. Abernathy, and S. J. Pearton, *Appl. Phys. Lett.* **82**, 4749 (2003).
- ¹³Y.-J. Zhao and A. J. Freeman, *J. Magn. Magn. Mater.* **246**, 145 (2002).
- ¹⁴S. Picozzi, Y.-J. Zhao, A. J. Freeman, and B. Delley, *Phys. Rev. B* **66**, 205206 (2002).
- ¹⁵Y.-J. Zhao and A. Zunger, *Phys. Rev. B* **69**, 104422 (2004).
- ¹⁶P. Mahadevan and A. Zunger, *Phys. Rev. Lett.* **88**, 047205 (2002).
- ¹⁷J. Ihm, A. Zunger, and M. L. Cohen, *J. Phys. C* **12**, 4409 (1979).
- ¹⁸D. Vanderbilt, *Phys. Rev. B* **41**, 7892 (1990).
- ¹⁹J. P. Perdew and Y. Wang, *Phys. Rev. B* **45**, 13244 (1992).
- ²⁰G. Kresse and J. Hafner, *Phys. Rev. B* **47**, 558 (1993); G. Kresse and J. Furthmüller, *ibid.* **54**, 11169 (1996).
- ²¹H. J. Monkhorst and J. D. Pack, *Phys. Rev. B* **13**, 5188 (1976).
- ²²Although e and t_2 levels in chalcopyrites split due to the tetragonal structure, we still use the tetrahedral nomenclature for discussing similarity with Mn in III–V. As shown in Fig. 1, the spin-up t_2 level of CuGaSe₂:Mn split by 1.7 eV into $t_a = d_{xz}; d_{yz}$, and $t_b = d_{xy}$ at Γ point, whereas the splitting of e and spin-down t_2 levels are not remarkable.
- ²³P. Mahadevan and A. Zunger, *Phys. Rev. B* **69**, 115211 (2004).
- ²⁴B. Sanyal, O. Bengone, and S. Mirbt, *Phys. Rev. B* **68**, 205210 (2003).
- ²⁵A. Zunger, *Solid State Phys.* **39**, 275 (1986).
- ²⁶R. M. White, *Quantum Theory of Magnetism* (McGraw–Hill, New York, 1970).
- ²⁷M. van Schilfgaarde and O. N. Mryasov, *Phys. Rev. B* **63**, 233205 (2001).